Applied Thermal Engineering 220 (2023) 119685

Contents lists available at ScienceDirect

Applied Thermal Engineering

journal homepage: www.elsevier.com/locate/ate

Research Paper

Leveraging look-ahead information for optimal battery thermal management

Alberto Broatch, Benjamín Pla *, Pau Bares, Augusto Perin

CMT-Motores Térmicos, Universitat Politècnica de València, Camino de Vera s/n, 46022 Valencia, Spain

ARTICLE INFO

Keywords:
Battery
Derating
Prediction

ABSTRACT

The efficiency and range of electric vehicles (EVs) is an actual object of concern among manufacturers. The fast market share growth together with issues such as range anxiety demand evermore robust battery thermal management system (BTMS) controllers to maximize its electrical output capability. Current rule-based controllers often cannot cope with the high variability of energy demand from EVs, leading to oscillations where derating occurs and increasing the EV overall energy consumption. This study proposes a prediction horizon estimation of the future energy demand based on driven cycles. Together with a look-ahead algorithm, it is possible to keep track of an optimal battery temperature which avoids battery derating during the warm-up phase of the vehicle. A battery temperature estimation using a probability matrix based on a Markov chain is proposed in which the controller improves its estimations by repeating the same route over several trips. Results show that the method can minimize the use of the electric battery heater by predicting the necessary battery temperature over a prediction horizon. Therefore, up to 4% of overall energy consumption is saved when the EV performs a daily commute driving cycle, when compared to the original controller. Also, a learning method is implemented, improving the future estimations by storing route data as more cycles are performed.

1. Introduction

As the market share of battery electric vehicles (BEVs) increase, as well as the batteries capacity, the concerns with extending range also increase, demanding clever controller architectures in order to optimize its usage. BEV autonomy can be severely affected by extreme weather conditions, leading to reductions above 50% in the driving range due to the air-conditioning and heating [1,2]. Therefore, approaches targeting the battery operation in cold climate have been studied such as thermal encapsulation and thermal uniformity [3,4].

In that scenario, battery thermal management (BTM) become utterly important since its effectiveness in controlling the battery temperature operation reflects on both energy and safety issues [5]. Lithium-Ion batteries have limited power output in cold temperatures due to higher internal resistance and suffer from premature ageing when operate at high temperatures, that could lead to a thermal runaway when overheated [6,7]. In this aspect, [8] have demonstrated through simulations that a proper BTM may reduce the probability of a thermal runaway event while increasing performance and lifetime of the battery pack.

There are many BTM architectures available for BEV. They can be roughly split into air-cooling and liquid-cooling systems and can also have indirect or direct-cooling strategies. Air-cooling BTM systems are generally simpler, low-maintenance and cheaper to be produced. However, they lack controllability and does not provide the efficiency of modern liquid-cooling BTM systems due to lower heat transfer capacity [9]. In addition, [10] shows with numerical simulation that a liquid-cooled architecture provide a more uniform thermal distribution, especially during high power demands. Others, rely on phase change materials (PCM) for BTMS since these materials can store large amounts of heat by changing phase without changing its temperature [11]. Novel materials and also hybrid cooling system with PCMs have been studied and show promising results [12,13].

Differently from hybrid electric vehicles (HEV) and internal combustion engines (ICE), the BEV lacks a thermal source since there is no heat reservoir, making the BTM on cold situation challenging. Heating, ventilation and air-conditioning (HVAC) systems within EVs represent one of the major loads to the batteries, consuming up to 30% [14] and since they are highly related to the cooling/heating of the battery pack they are a key system to be optimized with the BTM being integrated in the direct-cooling strategies [15]. Besides the poor efficiency of the HVAC when operating as a heat pump (HP), there is ongoing development on coupling the HVAC machine together with conventional battery heaters, such as positive temperature coefficient heater (PTC) and electrical heaters [16].

Actual state-of-the-art thermal management controllers are rule-based. In one hand, besides tracking fairly effectively the battery temperature set, they struggle to cope with sharp oscillations in power

* Corresponding author.
E-mail address: benplamo@upv.edu.es (B. Pla).

https://doi.org/10.1016/j.applthermaleng.2022.119685
Received 7 June 2022; Received in revised form 21 October 2022; Accepted 15 November 2022
Available online 28 November 2022

Nomenclature

T_a	Ambient Temperature (°C)
P_b	Battery Power (kW)
T_b	Battery Temperature (°C)
P_c	Compressor Power (kW)
Q_b	Heat from battery (kW)
Q_{dch}	Heat from battery discharge (kW)
Q_{ht}	Heat from HT circuit (kW)
Q_m	Heat from motor (kW)
S	Position (km)
H	Hamiltonian

Abbreviations

ANN	Artificial Neural Network
BEV	Battery Electric Vehicle
BTM	Battery Thermal Management
BTMS	Battery Thermal Management System
CAV	Connected and Automated Vehicle
CPM	Cumulative Probability Matrix
DP	Dynamic Programming
ESO	Extended State Observer
EV	Electric Vehicle
FSMPC	Finite-set-based Model Predictive Controller
HIL	Hardware-in-the-loop
HT	High Temperature Circuit
HVAC	Heating, Ventilation and Air Conditioning
ICE	Internal Combustion Engine
LT	Low Temperature Circuit
MPC	Model Predictive Controller
NMPC	Non-linear Model Predictive Controller
OCP	Optimal Control Problem
PCM	Phase Change Materials
PH	Prediction Horizon
PI	Proportional–Integral Controller
PMP	Pontryagin's Minimum Principle
SOC	State-of-Charge
UDDS	Urban Dynamometer Driving Schedule
US06	US06 Supplemental Federal Test Procedure

Greek Letters

γ	Linear model coefficient
β	Weighting term
λ	Lagrange-multiplier co-state

Subscripts

a	Ambient
b	Battery
c	Compressor
dch	Discharge
ht	High temperature circuit
k	Discrete step
m	Motor

Superscripts

sp	Set-point

demand, possibly leading to overshoots in battery temperature. Furthermore, rule-base controllers spend a large amount of energy during warm-up phases to ensure that derating will not occur, thus offering room for improvement. On the other hand, control methods often rely on predictions of the future states to take better decisions of the control actuators of the system in order to minimize the parameters that matter the most. For instance, reducing the total energy consumed to heat or cool the battery pack or to minimize its deviation from a set-point can be done in advance whereas PID controllers cannot. In this sense, [17] proposes a fuzzy-logic controller during low temperature conditions by limiting the battery current to extend battery lifetime.

With the nowadays further availability of information from both the environment and from other vehicles, connected and automated vehicle (CAV) can take advantage of these data in order to predict future power demands, velocity profiles, road characteristics, and so on [18]. This opens a gap for implementing predictive controllers with high potential to save energy, increase range and also fulfil comfort requirements while keeping the operation conditions of batteries in a safety margin.

Extensive research has been approaching different manners to actively deal with the BTM. For instance, [19] has used artificial neural networks (ANN) to predict the battery temperature evolution using phase change materials (PCMs) as the BTMS. Other global optimization methods have also been employed, such as dynamic programming (DP), which was investigated by [20,21], who have developed an iterative DP algorithm to be able to implement the BTMS into a real-time controller, achieving significant energy reduction compared to the conventional BTM method.

Several other works rely on model predictive controllers (MPCs) to track the future battery temperature evolution and thus obtaining an optimal control sequence to act on the BTMS. [22] investigates the use of a non-linear model predictive controller (NMPC) to optimize the air conditioning machine. To cope with the non-linearity and the time variant nature of the thermoelectric battery models, [23] developed a finite-set-based MPC (FSMPC) with the addition of an extended state observer (ESO) to estimate and compensate the inherent prediction error. Hardware-in-the-loop (HIL) validation showed up to 30% energy improvement. Authors in [24] split the optimization of their work into two layers. The upper layer being responsible for creating a battery temperature trajectory based on a integrated cost function of cooling power and vehicle speed. Afterwards, a lower layer composed of a MPC tracks the cabin and battery temperatures references while minimizing energy consumption. For a UDDS cycle up to 10% energy saving was achieved.

In this paper, a predictive control strategy is proposed to optimize the warm-up phase of an EV over a real driving cycle. The goal is to reduce the total energy consumption of the integrated cooling system while keeping the battery temperature within an optimal temperature range to avoid derating. Although many articles employ prediction models and MPCs to control battery temperature [25,26], this work brings the novelty of estimating a variable battery temperature set-point T_b^{sp} based on stored in-vehicle driving cycles. Disturbances in prediction are often addressed as known variables from a known driving cycle. However, this work proposes an estimation of the real driving cycle disturbances by learning over different trips.

The present work will be divided into the following: A methodology explaining the system model and the prediction model development, results obtained from the proposed estimation evolution and conclusions of the effectiveness of the approach.

2. Materials and methods

2.1. Case study

This study presents a BTMS for a daily route between city and countryside, with urban and highway traffic. Assuming that every

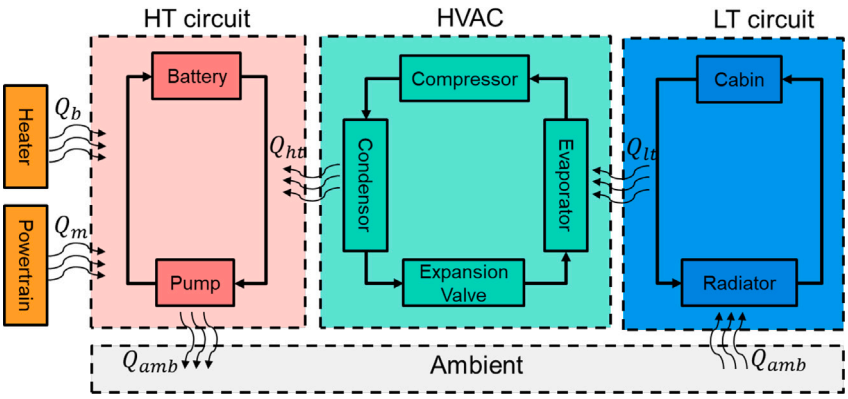

Fig. 1. Simplified representation of the plant model using the GTpower plant model when operated in heating mode. Heat is taken from the ambient from the LT circuit and driven to the HT circuit by the heat pump.

journey starts at a very low temperature scenario, such as −10 °C, the goal is to minimize the energy consumption by maintaining an optimal operating temperature of the vehicle's battery, this way preventing derating.

2.2. Plant description

In order to evaluate the control proposal, a GT-Power HVAC template is used as the plant model. This system model contains an electric vehicle (EV) liquid cooling system with a high temperature (HT) and low temperature (LT) coolant circuits, heat-pump/air-conditioning machine and a cabin model. In addition, all the vehicle dynamics are included within the model. An example of the described plant can be seen in Fig. 2. In this model, both battery and powertrain are regarded as heat nodes, which can transfer heat with their respective coolant circuits. The HVAC can operate both as a heat pump or air-conditioning.

During heating mode, heat is taken from the ambient and driven to the condenser placed at the HT circuit. The HT circuit also receives the dissipated heat from the powertrain, which is always connected to it. When in cooling mode, the cabin comfort is reached by removing heat of the LT circuit, in which the cabin is connected to, and releasing it to the ambient. Battery and cabin can also be heated in a direct manner, which consists of an electric heater connected to both elements.

The original system is composed by rule-based control actions and PIs to track the desired set-point. It is composed of tables that according to the ambient temperature define the actuators to heat or to cool the system. For this case, when at a −10 °C ambient temperature, the system is set to track a 22 °C battery temperature. Although having more details such as other actuators, valves, pumps and by-passes that control the flow and interaction between HT and LT circuits, Fig. 1 presents the concept of the plant for the sake of simplicity. Heat exchange parameters, coefficients and pump and compressor maps are the default of the template.

The only added block was a Simulink–GTPower connection, so the control sequence obtained from this study can by-pass the original PI controller. Therefore, the model is simulated to acquire input, output and state variables. These simulations provide data to evaluate the performance of the actuator on the state and thus choose the most effective variables to implement in the controller, which will be used in Section 2.3.

2.3. System model

In order to have a simple representative model of the complex one-dimensional model of the plant, a linear model is developed by identifying parameters which approximate both systems. In this case, the physical model is translated to a set of variables and parameters that correlates to the original system. The model is constructed in the discrete-time basis and have a single state, whose dynamics are modelled as:

$$T_{b_{k+1}} = T_{b_k} + \gamma_1 T_{b_k} + \gamma_2 Q_{b_k} + \gamma_3 P_{b_k} + \gamma_4 P_{c_k} - \gamma_5 T_a \quad (1)$$

where T_b, Q_b, P_b, P_c and T_a represents the battery temperature (in °C), the heat from the electric heater (in kW), the internal heat dissipated from the battery (in kW), the compressor power (in kW) and the ambient temperature (in °C), respectively. Sub-index k represents the current time-step and γ_j are the calibration coefficients that adjust the model to the plant. In this case, T_b stands for the state, Q_b acts as the control input and P_b and P_c measured disturbances to the system.

Table 1
Model coefficients.

Coefficient	Value [–]
γ_1	−2.9486e−04
γ_2	0.0014
γ_3	4.3492e−06
γ_4	0.0077
γ_5	2.0233e−04

The election of the linear model presented in Eq. (1) is based on physical intuition, since P_c has a direct impact on the heat from the condenser of the HVAC machine (Q_{ht}). Term P_b can lump both the heat dissipated from the powertrain into the HT circuit (Q_m) and with the heat dissipated from the internal resistance of the battery (Q_{dch}), since the power request from the powertrain directly correlates the electrical current of the battery, affecting the battery heat dissipation from its internal resistance. A last term T_a accounts for the heat rejection to the ambient. Despite the simplification to the model, the validation of the model regarding the actual temperature evolution showed little discrepancy between models. At last, those three terms are chosen since they have the major impact on the battery temperature evolution.

The model coefficients, γ_1, γ_2, γ_3, γ_4, γ_5 are identified by solving a system of linear equations with the plant parameters listed before, minimizing the model error with respect to the system plant in a set of tests. It consisted in exciting the plant model with random input heat rates (with Q_b) at a sample of 0.1 Hz. This way, the parameters of the linearized model are presented in Table 1.

Fig. 3 shows the validation of the prediction model for three different battery heater inputs, Q_b = [0, 3, 6] kW, over a US06 driving cycle. Comparing the temperature evolution with the high complexity GT-Power model, it can be assumed that the identified linear model of the system can reproduce the results with low deviation. Note that despite small differences in Fig. 2, these results have been obtained by simulating the complete cycle without any feedback of the actual battery temperature. In the proposed control application, there will be feedback of the current temperature and the error will be reduced.

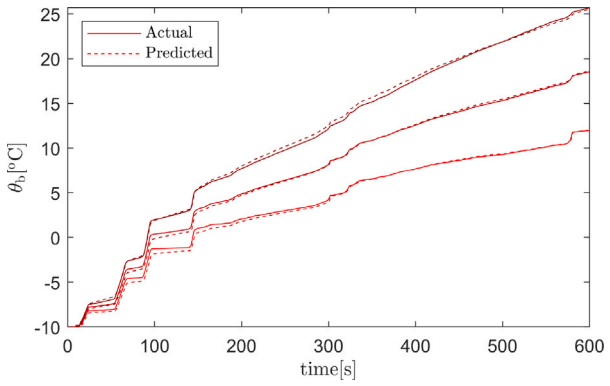

Fig. 2. Temperature evolution of the plant model and the linearized model for 3 different battery heater inputs over a US06 driving cycle.

2.4. Optimal control problem analysis

In this section an optimal control problem (OCP) is formulated from the dynamics of the system. Let us consider the following general dynamics of the system:

$$x_{k+1} = f(x_k, u_k, k) \tag{2}$$

where x_k is the state variable and u_k is the control action, and the function f allows to compute the state in a given time-step $(k+1)$ provided its previous values and actions. Consider also a cost L to be minimized along a prediction horizon (PH)

$$J = \sum_{i=1}^{PH} L(x, u, k) \tag{3}$$

In the case at hand, the system state (x) is the battery temperature T_{b_k}, the generic control action (u) is the battery heater power Q_{b_k} and the state function f represents Eq. (1). Concerning the cost L, also known as Lagrangian, the present work will consider the cost of heating the battery Q_{b_k}. To avoid battery derating, a term weighting the deviation between the actual battery temperature and that required to avoid derating is included in the cost function. Then, the battery temperature $T^{sp}_{b_k}$ is a value that can only be higher or equal to the actual battery temperature T_{b_k} and the Lagrangian may be defined as

$$L(x, k) = Q_{b_k} + \beta(T_{b_k} - T^{sp}_{b_k})^2 \tag{4}$$

In order to solve the OCP described above, the problem is initially solved analytically. According to Pontryagin's Minimum Principle (PMP) [27], the Lagrangian should be adjoined with the equation of the system dynamics (1) by introducing a co-state λ, leading to the Hamiltonian H that can be expressed as

$$H(x_k, u_k, \lambda_k, k) = L(x_k, u_k, k) + \lambda^T_{k+1} f(x_k, u_k, k) \tag{5}$$

where for the current work, Eq. (5) can be rewritten considering the states of the problem

$$H = Q_{b_k} + \beta(T_{b_k} - T^{sp}_{b_k})^2 + \lambda^T_{k+1}(\gamma_1 T_{b_k} + \gamma_2 Q_{b_k} + \gamma_3 P_{b_k} + \gamma_4 P_{c_k} + \gamma_5 T_{a_k}) \tag{6}$$

Also, the differential equation of the co-state variable can be derived:

$$\dot{\lambda} = -\frac{\partial H}{\partial x_k} = 2\beta(T^{sp}_{b_k} - T_{b_k}) + \lambda_k \gamma_1 \tag{7}$$

From (PMP), the optimal control input u^* is the one that minimizes the Hamiltonian function [28]. Analysing Eq. (6), it can be noticed that H is linear with the control action Q_b. Therefore, the Hamiltonian will only depend on the slope of this term, such that the optimal control will occur at both the extremes, being the minimum value when the slope is positive and the maximum value when the slope is negative. Hence, the actuation is limited between 0 and the maximum rated power of 6 kW.

The previous statements lead the OCP to be regarded as the so-called bang–bang control. In this case, the optimal control is either to heat at maximum power until reaching the battery temperature reference or do not heat. Also, the system can be said to be undetermined, which will be discussed later

$$u^*_k = \begin{cases} \bar{Q}_b & if \quad \lambda < \frac{-1}{\gamma_2} \\ undertermined & if \quad \lambda = \frac{-1}{\gamma_2} \\ 0 & if \quad \lambda > \frac{-1}{\gamma_2} \end{cases} \tag{8}$$

where γ_2 is a real and positive value and $\bar{Q}_b$ stands for the maximum rated power of the electric heater. However, as being treated as a bang–bang control, the solution oscillate between the extremes of the control action, being ruled by the evolution of the co-state λ. The times that the optimal control switches from maximum to minimum heat, i.e. switching time, are often a complex task to determine. In this particular case, it seems more natural to find a switching temperature instead of a switching time or value of lambda. As the minimum value of Q_{b_k} is 0, i.e. the system is not able to cool the battery, the battery set-point temperature is only meaningful if its value is above the current battery temperature. Then, according to the Lagrangian equation (4), the error difference between the actual state to the set-point state is a non-negative value, since the $T^{sp}_{b_k}$ is always higher or equal to the actual battery temperature. Therefore, this analysis induce to a case where Eq. (7) is positive ($\dot{\lambda} > 0$) in which leads to:

$$T_{b_k} \leq T^{sp}_{b_k} + \frac{\lambda \gamma_1}{2\beta} \tag{9}$$

$$\lambda \geq \frac{(T_{b_k} - T^{sp}_{b_k})2\beta}{\gamma_1} \tag{10}$$

Therefore, during heating, a new expression is formulated that correlates with the costate λ and also an expression that disclose the switching function as a function of the battery temperature T_{b_k}

$$\frac{(T_{b_k} - T^{sp}_{b_k})2\beta}{\gamma_1} \leq \lambda < \frac{-1}{\gamma_2} \tag{11}$$

$$T_{b_k} < T^{sp}_{b_k} - \frac{\gamma_1}{2\beta\gamma_2} \tag{12}$$

However, it is noticeable that there is a case where the solution is undetermined when the co-state matches the equality ($\lambda = \frac{-1}{\gamma_2}$). In this case, the system is said to be on a singular arc and the control will assume values between the control constraints. While the solution in this situation cannot be obtained from the analysis of the Hamiltonian, in this case, it is considered that the control will be a value of Q_b that minimizes $(T_{b_k} - T^{sp}_{b_k})$, such that

$$u'_k = \left[(T^{sp}_{b_k} - T_{b_k}) - \gamma_1 T_{b_k} - \gamma_3 P_{b_k} - \gamma_4 P_{c_k} - \gamma_5 T_{a_k}\right] \frac{1}{\gamma_2} \tag{13}$$

And thus the optimal control action can be expressed as:

$$u^*_k = \begin{cases} \bar{Q}_b & if \quad u'_k > \bar{Q}_b \\ u'_k & if \quad 0 < u'_k < \bar{Q}_b \\ 0 & if \quad u'_k < 0 \end{cases} \tag{14}$$

This analysis show that the current rule-based control embedded in the system, consisting in using maximum heating until the battery set point temperature (in the case at hand 22 °C) is reached, is almost optimal for the actual set-point defined within the controller, specially if the value of β is high. Nevertheless, it is possible to further optimize the controller by defining a sequence of $T^{sp}_{b_k}$ which avoid battery derating by taking advantage of the look ahead information, instead of using a constant set point of 22 °C as done by the current rule-based control.

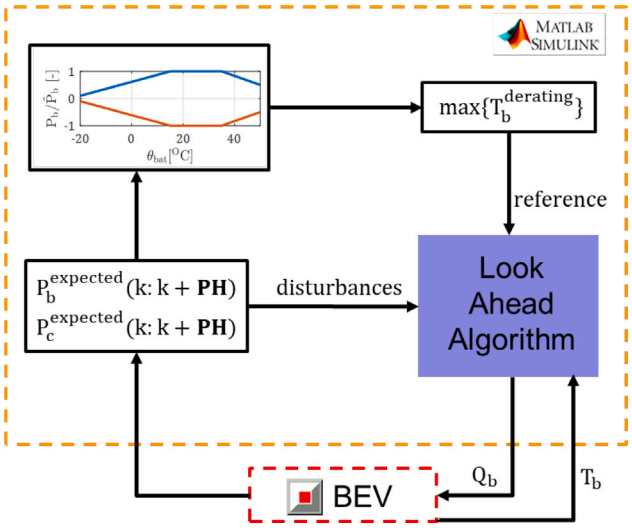

Fig. 3. Overall schematics of the Simulink/GT-Power connection with the look-ahead algorithm. Power predictions act as disturbances to the system and the reference battery temperature is calculated from the derating function.

2.5. Proposed solution

As stated in the previous paragraph, given a temperature set-point $T_{b_k}^{sp}$, the standard rule-based controller is almost optimal for the actual system modelling of this study. Therefore, the current study proposes a look-ahead temperature set-point, by taking advantage of the route information from past driving cycles. It consists on using the expected power demand of the driving cycle to estimate $T_{b_k}^{sp}$ from the battery curve relating its maximum power with the battery temperature. This way, a temperature set-point that avoid derating can be forecast based solely on the expected power demands.

To simulate the controller with the system plant, a Simulink-GT-Power connection is performed using a S-Function Simulink block, which applies the optimal control sequences to the GT-Power model. A schematic of the control system is demonstrated in Fig. 3. It can be seen that the controller uses the sensors measurements as disturbances and also as the input for a derating map, which provides the optimal reference temperature. With this information the controller can provide the control sequence to the GT-Power model that return the measured output back to the controller.

However, one cannot have the future power demands in advance, so a method is implemented to have an estimation of this data beforehand. It consists in a route estimation where the controller can learn the trip by repeating it during several days. To do so, a first trip is performed using the original rule-based controller, recording the outputs of the system such as P_b and P_c. These outputs are used as input disturbances for the next unknown round trips.

2.5.1. Power demand prediction

To predict the power demand from the battery P_b and the compressor power P_c, the proposed solution uses a Markov chain to estimate the future demands due to its simplicity to represent an unknown system based solely on the past states to project the future states. In this case, being the P_{b_k} and P_{c_k} the current states, and the actual position in the route S_k. This prediction algorithm is based on previous works by the authors in [29,30]. In order to account the characteristics of each part of the cycle, e.g. high and low power demand, we split the cycle into segments of 1 km length using the information of the previously recorded driving commutes. Therefore, the Markov chain is the sequence of random values $P_{b_1}, P_{b_2}, \dots, P_{b_k}$ and $P_{c_1}, P_{c_2}, \dots, P_{c_k}$, whose probability can be expressed as

$$P(Pb_{k+1} = p_{b_k+1} | P_{b_1} = p_{b_1}, \dots, P_{b_k} = p_{b_k})$$

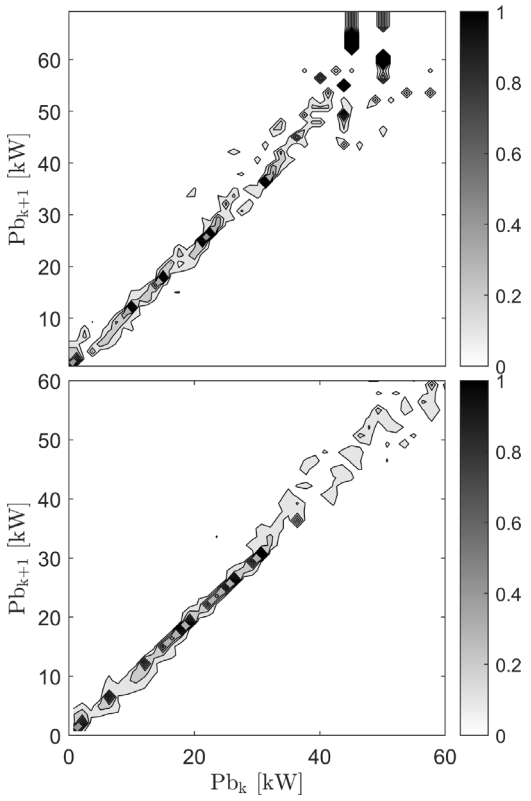

Fig. 4. Transition probabilities from current battery power P_{b_k} to $P_{b_{k+1}}$ after 1 cycle on the top and after 9 cycles on the bottom.

$$= P(Pb_{k+1} = p_{b_k+1} | P_{b_k} = p_{b_k}) \tag{15}$$

$$P(Pc_{k+1} = p_{c_k+1} | P_{c_1} = p_{c_1}, \dots, P_{c_k} = p_{c_k}) = P(Pc_{k+1} = p_{c_k+1} | P_{c_k} = p_{c_k}) \tag{16}$$

where p_{b_k} and p_{c_k} stand for possible values of P_b and P_c. Being $P_{x_k+1} = i$ – with x representing both battery and compressor – the future state at step $k+1$, provided that the present state $P_{x_k} = j$, the probability of being in a future state i at step $k+1$ can be estimated as the ratio between the number of times the future state have occurred if the previous state is the present state, herein called N_{ij}, by the number of all possible states, such that

$$P(Px_{k+1} = i | P_{x_k} = j) = \frac{N_{ij}}{\sum_j N_{ij}} \tag{17}$$

A transition matrix is created with the expression above, which can be seen in Fig. 4, storing the probability of transition of any state j to i. The bottom plot show how the probability evolves after the eighth trip have been stored. Afterwards, a cumulative probability matrix (CPM) is constructed, since the sum of all probabilities leaving a state must equals 1, by integrating every row of the transition matrix. Hence, at every time-step, the next P_x will be chosen by taking a random number and extract the closest value from the CPM. It is important to point out that for this study we assume that the vehicle, in the case at hand the GTPower plant model, can provide a feedback of the actual battery power demanded and the actual position.

The analysis consists in two parts. First, the sensitivity of the prediction horizon is evaluated by varying the length of future forecast. Then, after choosing the horizon that best suits the problem, the impact of estimating the route by learning is analysed.

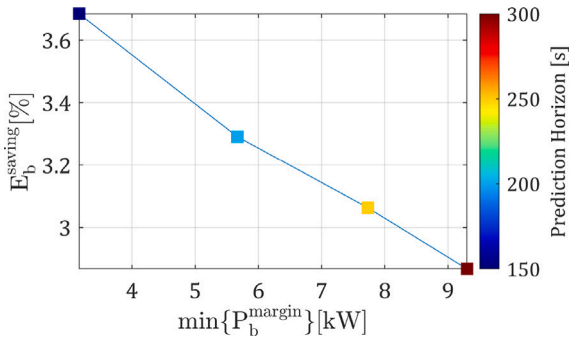

Fig. 5. Influence of the prediction horizon on both the overall energy savings against and the power reserve margin.

3. Results and discussion

3.1. Prediction horizon evaluation

As stated before, the aim of this study is to control the battery temperature to reach a given value to avoid derating and thus increasing the vehicle range. By doing so, it is possible to reduce the overall energy consumption when operating the EV during the warm-up phase by controlling the battery heater contained in the plant model. That being said, the effectiveness of the predictive controller, regards heavily on the horizon chosen for the controller. To investigate this parameter, simulations were run with different PH such that $PH = [150, 200, 250, 300]$.

Fig. 5 presents the results for the PH horizons as a function of the overall energy savings and the power reserve to avoid derating. It can be seen that there is a compromise between the safe gap of power available and the amount of energy that is saved from the controller. Shorter prediction horizons in this case only forecast the battery temperature demanded at the beginning of the cycle, which required less heat to be added to the HT circuit, thus saving more energy. On the other hand, this savings result in a smaller gap between the maximum power available and the required power from the battery, becoming a risky operation where deviations from the model could lead to derating. However, when longer prediction horizons are considered, this risk is minimized at the cost of further heating the battery, this way consuming more energy.

3.2. Optimal control comparison

With the battery temperature set-point $T_{b_k}^{sp}$ in a PH, the controller can track this temperature, which is the minimum temperature necessary to avoid derating for the given power demand. In order to evaluate the profits of our current solution, presented in 2.4, a DP tool as the controller is investigated. Using the same battery temperature model (1), with the same coefficients from Table 1, the results show that as the decision to heat or not the coolant system relies on the battery temperature set-point within the PH.

However, as the DP needs to be run before the cycle, only the control sequence is applied to the simulation. Considering that the model has full access to the cycle information before-hand, Fig. 6 shows that the DP solution can bring better energy management compared to the look-ahead controller once the controller minimizes the power margin available by reducing the electric heater Q_b use. A 5.5% in energy reduction could be obtained with DP against a 3.3% with the look-ahead algorithm. This can be explained as the DP solution brings a very small power margin, of 1.5 kW compared to the 5.7 kW of the look-ahead algorithm. However, although being optimal, the DP solution does not consider the deviations from the T_b evolution, which

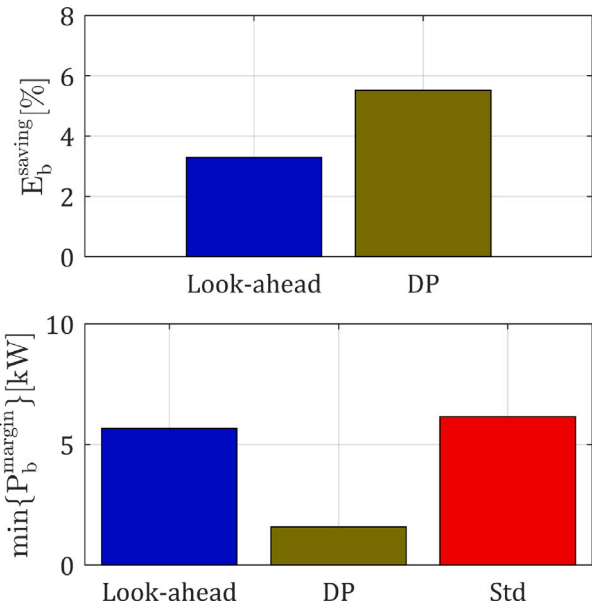

Fig. 6. Energy savings and power reserve margin with the look-ahead algorithm, with a DP solution and with the standard PI controller.

in a real-case, without receiving the feedback of the current state, would lead the solution to a derating event.

As the look-ahead algorithm receives the feedback from the plant model every time-step k, it can keep track of the actual T_b and thus provide a better estimation of the $T_{b_k}^{sp}$. This would not be possible with the DP solution, once calculating it for every time-step k would have a high computational cost.

3.3. Route estimation evaluation

For this part of the analysis, a PH of 200 s is taken from the previous section, by choosing a compromise between the potential energy saving and the power reserve margin. With this PH, a simulation for the learning algorithm is executed, where eight real-driving cycles are simulated in a row to evaluate the potential benefit of this approach. A first simulation is run without any control applied to the system, besides its original rule-based controller. Then, the gathered power requirements of the vehicle, P_b and P_c, are stored and feed the probability matrix to provide the disturbances to the second cycle and so on.

Fig. 7 displays the evolution of T_b, Q_b and P_b. The electric heater Q_b is activated at the beginning of the cycle since the whole system is at −10 °C and the battery power demand forecast tells that within the PH the battery needs to be heated. After 200 s, the battery temperature is almost at the set-point, with the controller not detecting derating in the forecast. Therefore, Q_b is turned off for the rest of cycle and the battery heating is made only due to its own internal resistance and heat exchange between battery and HT circuit. It can be highlighted that derating could be avoided for all simulations, by taking advantage of the battery power estimations, even though each cycle have an unknown power demand. With the proper battery temperature set-point, the time actuating on the electric heater is considerably lower than the standard controller, which can be noticed on the final state-of-charge (SoC) difference.

It is expected that lower battery temperatures will be reach, since the original controller aims to heat the battery up to 22 °C, and the dynamic temperature set-point here proposed are smaller. However, much of this heat is not necessary since derating can be avoided by heating only the sufficient to avoid derating. Fig. 8 shows that as the simulations goes on, all the cycles performed maintained a safe power

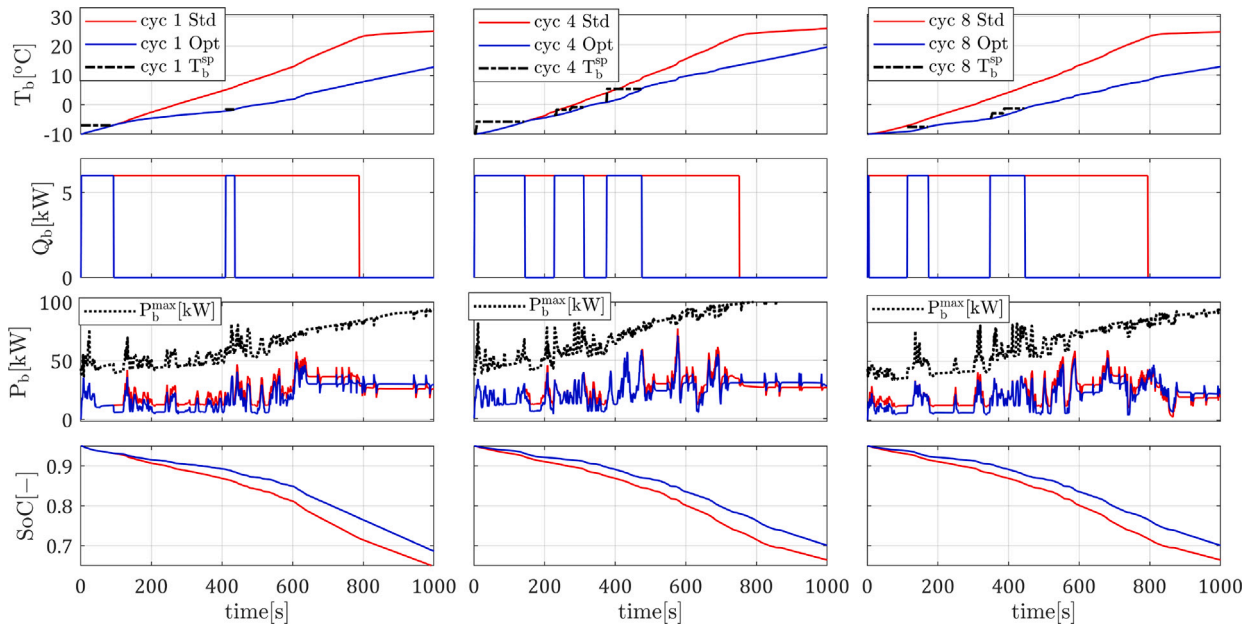

Fig. 7. Results of the battery temperature evolution, electric heater power, battery power demand with the maximum limit and evolution of the state-of-charge over the route in the first, fourth, and last cycle of the learning algorithm evaluation.

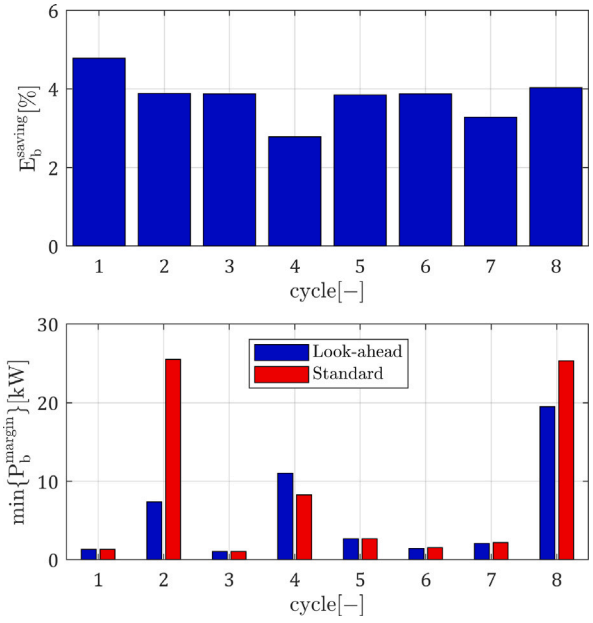

Fig. 8. Energy savings and power reserve margin evolution with the learning algorithm compared to the original controller over the nine daily commute.

margin but also reducing the overall energy consumption of the cycle. Up to 4% of energy savings were achieved for all cases, comparing to the original PI controller and derating have not occurred, since the power margin stayed always positive.

4. Conclusions

This paper addressed a problem where an EV departure from a −10 °C ambient temperature run a real-driving cycle of a daily commute. The goal was to optimize the warm-up phase by actuating on the battery electrical heater in order to avoid battery derating. A prediction model of the system was elaborated to forecast the future power demands and thus choose the best control sequence Q_b that minimizes the overall energy consumption. Two studies were done, being the first an evaluation of the sensitivity of the model by varying the prediction horizon and the second an application of the learning algorithm capable of adapting the EV power predictions. From the results, we can state that:

- A compromise between the energy savings and the battery power margin needs to be selected in order to avoid a derating condition while minimizing the energy consumption. Even though choosing a conservative PH, still over 3.5% of energy reduction can be achieved when comparing to the baseline rule-based control.
- The learning algorithm proved to be advantageous, since it improved the disturbances estimations cycle after cycle. In addition, it shows that an unknown route can be estimated with fairly good accuracy in the first simulations, sparing the need of costly prediction models and large datasets of information from the route.
- Up to 4% of overall energy reduction could be achieved – when compared to the original PI controller – without the occurrence of derating for all the cycles evaluated, maintaining a power reserve margin.

4.1. Future works

It could be noticed during the development of this study that further improvement to the BTMS could be achieved by modelling the response of the HVAC machine. A future work can take advantage of the compressor efficiency in order to predict the best control input. Furthermore, an approach such as the one presented in this paper could be implemented in a cabin thermal management, reaching comfort demands with lesser energy consumption.

CRediT authorship contribution statement

Alberto Broatch: Formal analysis, Writing – review & editing, Funding acquisition. **Benjamín Pla:** Conceptualization, Methodology, Writing – review & editing, Funding acquisition. **Pau Bares:** Conceptualization, Methodology. **Augusto Perin:** Software, Data curation, Writing – original draft.

Declaration of competing interest

The authors declare that they have no known competing financial interests or personal relationships that could have appeared to influence the work reported in this paper.

Data availability

No data was used for the research described in the article.

Acknowledgements

All authors have read and agreed to the published version of the manuscript.

Funding

This research has been partially funded by the Agencia Valenciana de la innovación, Spain through the project INNEST/2021/120, entitled "Demostrador Tecnológico de un paquete de baterías para vehículo eléctrico".

References

[1] M.A. Jeffers, L. Chaney, J.P. Rugh, Climate Control Load Reduction Strategies for Electric Drive Vehicles in Warm Weather, Vol. 2015-April, SAE International, 2015.
[2] M.A. Jeffers, L. Chaney, J.P. Rugh, Climate control load reduction strategies for electric drive vehicles in cold weather, SAE Int. J. Passeng. Cars - Mech. Syst. 9 (2016).
[3] A.R. Babu, B. Minovski, S. Sebben, Thermal encapsulation of large battery packs for electric vehicles operating in cold climate, Appl. Therm. Eng. 212 (2022) 118548.
[4] Z. Lei, Y. Zhang, X. Lei, Temperature uniformity of a heated lithium-ion battery cell in cold climate, Appl. Therm. Eng. 129 (2018) 148–154.
[5] T.M. Bandhauer, S. Garimella, T.F. Fuller, A critical review of thermal issues in lithium-ion batteries, J. Electrochem. Soc. 158 (2011).
[6] J. Vetter, P. Novák, M. Wagner, C. Veit, K.-C. Möller, J. Besenhard, M. Winter, M. Wohlfahrt-Mehrens, C. Vogler, A. Hammouche, Ageing mechanisms in lithium-ion batteries, J. Power Sources 147 (1–2) (2005) 269–281.
[7] M.-K. Tran, A. Mevawalla, A. Aziz, S. Panchal, Y. Xie, M. Fowler, A review of lithium-ion battery thermal runaway modeling and diagnosis approaches, Processes 10 (6) (2022).
[8] A. García, J. Monsalve-Serrano, R.L. Sari, S. Martínez-Boggio, Thermal runaway evaluation and thermal performance enhancement of a lithium-ion battery coupling cooling system and battery sub-models, Appl. Therm. Eng. 202 (2022).
[9] W. Wu, S. Wang, W. Wu, K. Chen, S. Hong, Y. Lai, A critical review of battery thermal performance and liquid based battery thermal management, Energy Convers. Manage. 182 (2019) 262–281.
[10] M. Akbarzadeh, T. Kalogiannis, J. Jaguemont, L. Jin, H. Behi, D. Karimi, H. Beheshti, J.V. Mierlo, M. Berecibar, A comparative study between air cooling and liquid cooling thermal management systems for a high-energy lithium-ion battery module, Appl. Therm. Eng. 198 (2021).
[11] A.R. Bais, D.G. Subhedhar, N.C. Joshi, S. Panchal, Numerical investigation on thermal management system for lithium ion battery using phase change material, Mater. Today: Proc. 66 (2022) 1726–1733, 2022 International Conference on Recent Advances in Engineering Materials.
[12] R. Jilte, A. Afzal, S. Panchal, A novel battery thermal management system using nano-enhanced phase change materials, Energy 219 (2021) 119564.
[13] M. Akbarzadeh, J. Jaguemont, T. Kalogiannis, D. Karimi, J. He, L. Jin, P. Xie, J. Van Mierlo, M. Berecibar, A novel liquid cooling plate concept for thermal management of lithium-ion batteries in electric vehicles, Energy Convers. Manage. 231 (2021) 113862.
[14] Z. Tian, C. Qian, B. Gu, L. Yang, F. Liu, Electric vehicle air conditioning system performance prediction based on artificial neural network, Appl. Therm. Eng. 89 (2015) 101–114.
[15] Z. Wang, L. Huang, F. He, Design and analysis of electric vehicle thermal management system based on refrigerant-direct cooling and heating batteries, J. Energy Storage 51 (2022) 104318.
[16] T. Zhang, C. Gao, Q. Gao, G. Wang, M.H. Liu, Y. Guo, C. Xiao, Y.Y. Yan, Status and development of electric vehicle integrated thermal management from BTM to HVAC, Appl. Therm. Eng. 88 (2015) 398–409.
[17] H. Min, Z. Zhang, W. Sun, Z. Min, Y. Yu, B. Wang, A thermal management system control strategy for electric vehicles under low-temperature driving conditions considering battery lifetime, Appl. Therm. Eng. 181 (2020).
[18] M.R. Amini, J. Sun, I. Kolmanovsky, Two-layer model predictive battery thermal and energy management optimization for connected and automated electric vehicles, in: 2018 IEEE Conference on Decision and Control (CDC), Vol. 2018-Decem, (Cdc) IEEE, 2018, pp. 6976–6981.
[19] F. Jaliliantabar, R. Mamat, S. Kumarasamy, Prediction of lithium-ion battery temperature in different operating conditions equipped with passive battery thermal management system by artificial neural networks, Mater. Today: Proc. 48 (2022) 1796–1804.
[20] C. Zhu, F. Lu, H. Zhang, J. Sun, C.C. Mi, A real-time battery thermal management strategy for connected and automated hybrid electric vehicles (CAHEVs) based on iterative dynamic programming, IEEE Trans. Veh. Technol. 67 (9) (2018) 8077–8084.
[21] S. Zhao, C.C. Mi, A two-stage real-time optimized EV battery cooling control based on hierarchical and iterative dynamic programming and MPC, IEEE Trans. Intell. Transp. Syst. 23 (8) (2022) 11677–11687.
[22] H. Wang, I. Kolmanovsky, M.R. Amini, J. Sun, Model predictive climate control of connected and automated vehicles for improved energy efficiency, in: 2018 Annual American Control Conference (ACC), Vol. 2018-June, IEEE, 2018, pp. 828–833.
[23] C. Zhu, F. Lu, H. Zhang, C.C. Mi, Robust predictive battery thermal management strategy for connected and automated hybrid electric vehicles based on thermoelectric parameter uncertainty, IEEE J. Emerg. Sel. Top. Power Electron. 6 (4) (2018) 1796–1805.
[24] Z. Shuofeng, M.R. Amini, J. Sun, C. Mi, A two-layer real-time optimization control strategy for integrated battery thermal management and HVAC system in connected and automated HEVs, IEEE Trans. Veh. Technol. 70 (7) (2021) 6567–6576.
[25] Y. Ma, H. Ding, Y. Liu, J. Gao, Battery thermal management of intelligent-connected electric vehicles at low temperature based on NMPC, Energy 244 (2022) 122571.
[26] I. Cvok, J. Deur, Nonlinear Model Predictive Control of Electric Vehicle Cabin Cooling System for Improved Thermal Comfort and Efficiency, Institute of Electrical and Electronics Engineers Inc., 2022, pp. 1759–1764.
[27] D.E. Kirk, Optimal Control Theory: An Introduction, Courier Corporation, 2004.
[28] A.E. Bryson, Applied Optimal Control: Optimization, Estimization and Control, Vol. 2, Hemisphere, 1975.
[29] J.M. Luján, C. Guardiola, B. Pla, V. Pandey, Impact of driving dynamics in RDE test on NOx emissions dispersion, Proc. Inst. Mech. Eng. D 234 (6) (2020) 1770–1778.
[30] H. Climent, B. Pla, P. Bares, V. Pandey, Exploiting driving history for optimising the energy management in plug-in hybrid electric vehicles, Energy Convers. Manage. 234 (2021) 113919.